File Revision Date :

December 8, 2025

Data Set Description:

PI:	Michaël Sicard
Instrument:	Elastic, backscatter lidar "LiO3T"
Site:	OPAR-StPaulMaido, Reunion island (21° S, 55° E, 2158 m a.s.l.)
Measurement Quantities:	Vertical profiles of particle backscatter coefficient at 532 nm (3-45 km) and linear particle depolarization ratio at 532 nm (3-25 km)

Contact Information:

Name:	Michaël Sicard
Institute:	LACy, UMR 8105 UR CNRS MF, Université de la Réunion
Adresse :	15, avenue René Cassin – CS 92003, 97744 Saint-Denis, France Cédex 9
Phone:	+262 2 62 52 89 63
Email:	michael.sicard@univ-reunion.fr

Instrument Description:

(See Figures 1 and 2) The emission consists in a Quanta Ray Pro 290 laser from Spectra-Physics emitting initially at 1064 nm at 30 Hz. While the fourth harmonic (266 nm) is used to retrieve tropospheric ozone profiles (through its passage in a Raman cell generating 289 and 316 nm pulses), we use the second harmonic (532 nm) to retrieve aerosol light extinction and backscattering. Each pulse at 532 nm provides an energy of 250 mJ. The laser beam diameter is of about 10 mm, and its divergence is about 0.5 mrad. The optical design of this lidar for aerosol measurements is represented in Figure 3. Again, the emission and reception of this lidar are located in different rooms, explaining the use of many mirrors. The lenses, BE1, BE2 and BE3, magnify the signal by a 15 factor. The final emitted beam diameter is 100 mm.

The reception is made of two telescopes: one for the Rayleigh and Raman channels (532, 607 and 1064 nm, respectively), and the other for the polarized channels at 532 nm. The first telescope (M500) consists in a 500 mm diameter primary mirror. An optical fiber located at its focal point, conducts the signal to the detection box. Dichroic filters separate the 532, 607 and 1064 nm wavelengths. The second telescope consists in a 200 mm diameter primary mirror immediately followed by a polarizing cube. An optical fiber leads the polarized and cross-polarized beams to interference filters and to the detectors.

All the detectors are PMT from Hamamatsu, except for the 1064 nm detector, which is an avalanche diode with a 3 mm diameter sensor. The 532 high energy channel (532H) detector is the only one electronically shuttered. All the acquisition cards are from Licel. The acquisition of the 532 nm polarized channel as well as the 607 nm channel are in photocounting mode. The acquisition of the 532H channel is in photocounting and analog modes, and the acquisition of the 1064nm channel is only in analog mode. Raw files follow a 2-minute integration.

Algorithm Description:

Data processing levels range from Level 0 to Level 2.

- Level 0 products (L0) are uncorrected and uncalibrated raw data files in Licel format at full resolution produced by the instrument.

- Level 1 products (L1) provide cloud-free data cleaned from any instrumental artifact (electronic parasites, synchronization problems, power disrupt, etc.). The cloud mask is currently manual. These corrections are essential for any user to be able to apply their own specific aerosol preprocessing without errors linked to the instrument itself or the weather.
- Level 2 products (L2) provide processed lidar data including: saturation correction, background-sky correction, geometrical form factor correction and gluing between high and low-energy channels (L2a). These products also provide the aerosol optical properties and their corresponding uncertainties (L2b).

Only L2b data are publicly available. Most important is the inversion method used. This dataset has been inverted with the two-component Klett inversion (Klett, 1981; 1985) assuming a constant lidar ratio of 50 sr. More details on Level 1 and 2 production can be found in Gantois et al. (2024). As far as the depolarization ratio is concerned, the Rayleigh calibration (cross and parallel) method (Behrendt and Nakamura, 2002) is used for data prior to 2017 and the 3-signal (total, cross and parallel) method (Reichardt et al., 2003) is used after 2017.

Expected Precision/Accuracy of Instrument:

The total uncertainty budget is described in Appendix B of Gantois et al. (2024) and summarized in Table 1. Four sources of uncertainty were propagated in quadrature (Sicard et al., 2009; Rocadenbosch et al., 2010): (i) uncertainty due to the Rayleigh calibration value, (ii) uncertainty due to the lidar ratio value with a distinction between LR, top and LR, bottom defining the respective upper and lower error bars, (iii) uncertainty due to the SNR vertical distribution, (iv) and uncertainty due to the SNR value at the calibration altitude.

The uncertainty analyses reveal a strong influence of the LR value in the low-altitude ranges and a strong influence of the SNR in the high-altitude ranges. Uncertainty values relative to the total backscatter coefficient are low. Uncertainty values relative to the aerosol backscatter coefficient are high because of the very low aerosol backscatter coefficient values generally observed above Maïdo observatory.

Instrument history and perspectives:

The OPAR LiO3T lidar delivers aerosol optical products (backscatter coefficients at 532 nm and linear particle depolarization ratios at 532 nm) since July 2014. The preprocessed (L1), processed (L2a) and inverted (L2b) data have been performed in an automated and harmonized manner. Uncertainties have been estimated following state-of-the-art formulations of lidar uncertainty budget. The lidar is operated two nights/week on Monday and Tuesday night from approximately 19 to 01:00 LT. During EarthCARE overpasses, measurements are extended until at least 04:00 LT. OPAR-StPaulMaido aerosol lidars are participating to EarthCARE cal/val exercise in the framework of ESA EVID 05 (ACTRIS-EU) and EVID 15 (ACTRIS-FR) projects. Data of this instruments have been used recently in Baron et al. (2023) and Sicard et al. (2025).

A new lidar called TAMARIN (Temperature Aerosol huMidity lidAr at Reunion IslaNd) is currently under development within the CNRS-INSU funded GON lidar project (2022-2025), aiming at a major upgrade and automation of the OHP and OPAR lidar parks. TAMARIN is designed to measure unmanned, unattended 7 nights/week the profiles of water vapor and aerosols. Elastic parallel, elastic perpendicular and Raman channels are planned at both 355 and 532 nm. TAMARIN should be included in the ACTRIS European research infrastructure and, as such, all optical products will be delivered by the Single Calculus Chain of ACTRIS. When all aerosol

products of TAMARIN are validated, only TAMARIN aerosol products will be sent to both ACTRIS and NDACC database.

Reference Articles:

Baron, A., Chazette, P., Khaykin, S., Payen, G., Marquestaut, N., Bègue, N., and Duflot, V.: Early Evolution of the Stratospheric Aerosol Plume Following the 2022 Hunga Tonga-Hunga Ha'apai Eruption: Lidar Observations From Reunion (21°S, 55°E), Geophys. Res. Lett., 50, e2022GL101751, https://doi.org/10.1029/2022GL101751, 2023.

Behrendt, A. and Nakamura, T.: Calculation of the calibration constant of polarization lidar and its dependency on atmospheric temperature, Opt. Express, 10, 805, https://doi.org/10.1364/OE.10.000805, 2002.

Gantois, D., Payen, G., Sicard, M., Duflot, V., Bègue, N., Marquestaut, N., Portafaix, T., Godin-Beekmann, S., Hernandez, P., and Golubic, E.: Multiwavelength aerosol lidars at the Maïdo supersite, Réunion Island, France: instrument description, data processing chain, and quality assessment, Earth Syst. Sci. Data, 16, 4137–4159, https://doi.org/10.5194/essd-16-4137-2024, 2024.

Klett, J. D.: Stable analytical inversion solution for processing lidar returns, Appl. Opt., 20, 211, https://doi.org/10.1364/AO.20.000211, 1981.

Klett, J. D.: Lidar inversion with variable backscatter/extinction ratios, Appl. Opt., 24, 1638, https://doi.org/10.1364/AO.24.001638, 1985.

Reichardt, J., Baumgart, R., and McGee, T. J.: Three-signal method for accurate measurements of depolarization ratio with lidar, Appl. Opt., 42, 4909, https://doi.org/10.1364/AO.42.004909, 2003.

Rocadenbosch, F., Md. Reba, M. N., Sicard, M., and Comerón, A.: Practical analytical backscatter error bars for elastic one-component lidar inversion algorithm, Appl. Opt., 49, 3380, https://doi.org/10.1364/AO.49.003380, 2010.

Sicard, M., Comerón, A., Rocadenbosch, F., Rodríguez, A., and Muñoz, C.: Quasi-analytical determination of noise-induced error limits in lidar retrieval of aerosol backscatter coefficient by the elastic, two-component algorithm, Appl. Opt., 48, 176, https://doi.org/10.1364/AO.48.000176, 2009.

Sicard, M., Baron, A., Ranaivombola, M., Gantois, D., Millet, T., Sellitto, P., Bègue, N., Bencherif, H., Payen, G., Marquestaut, N., and Duflot, V.: Radiative impact of the Hunga stratospheric volcanic plume: role of aerosols and water vapor over Réunion Island (21° S, 55° E), Atmos. Chem. Phys., 25, 367–381, https://doi.org/10.5194/acp-25-367-2025, 2025.

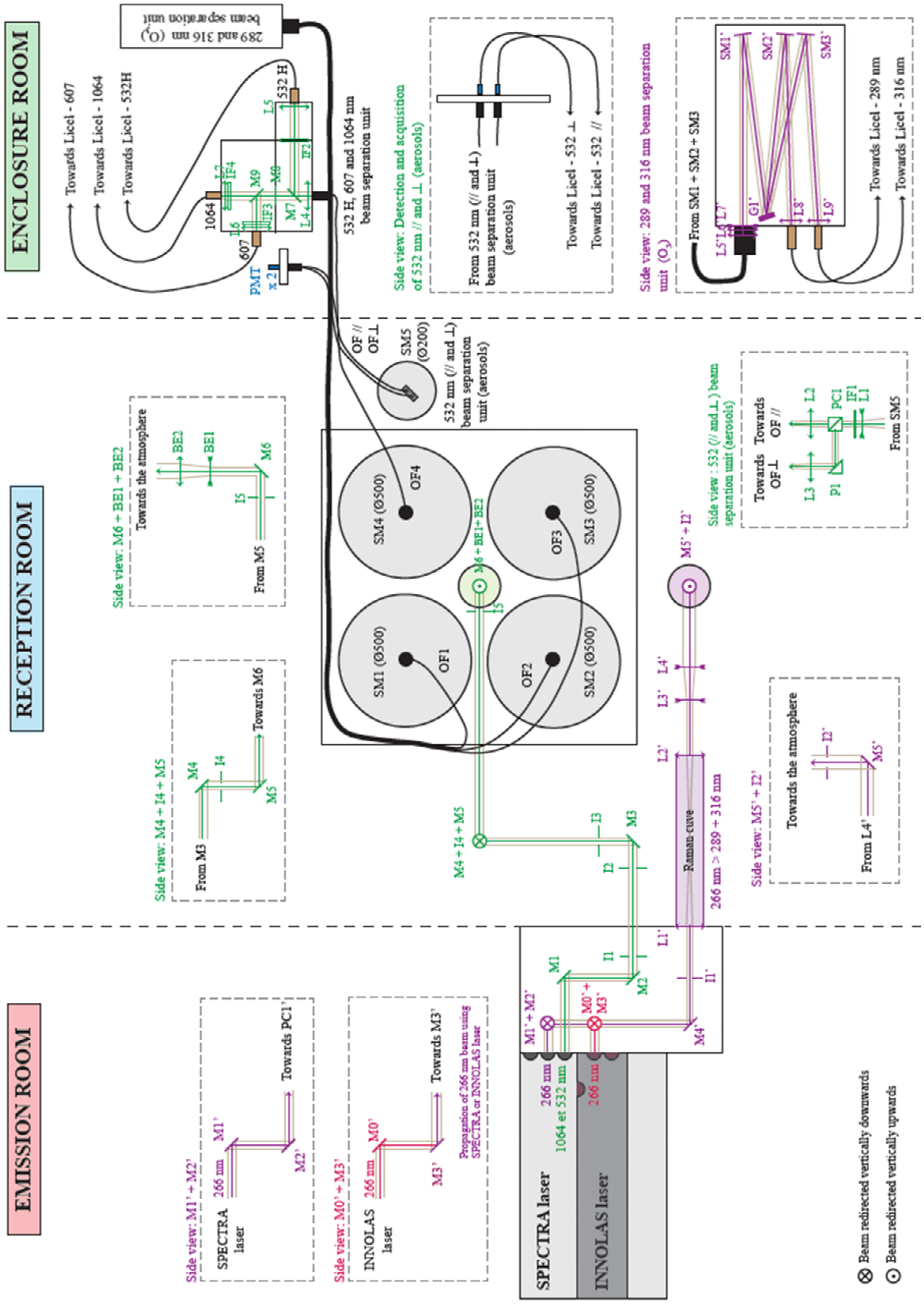

Figure 1: LiO3T optical scheme.

LiO3T	Id. Optical scheme	Type
Emission	M1, ..., M6	Rmax 532 and 1064 nm (ø= 1'')
	I1, ..., I5	Alignment iris
	BE1	Lens (f= -120 mm)
	BE2	Lens (f= +1650 mm)
	M0', ..., M3'	Rmax 266 nm (ø= 1'')
	M4'	Rmax 266 nm (ø= 38 mm)
	I1'	Alignment iris
	L1', L2'	Meniscus lens (ø= 21 mm, f= +746 mm)
	L3'	Biconcave lens
	L4'	Doublet lenses
	M5'	Rmax 266 nm (ø= 2'')
Reception	SM1, ..., SM4	Primary mirror (ø= 0.5 m, f= 1.5 m)
	SM5	Primary mirror (ø= 0.2 m, f= +1.06 m)
	OF1, ..., OF4	Optical fiber (ø= 1 mm)
	OF // and OF ⊥	Optical fiber (ø= 0.6 mm)
532 // and ⊥ beam separation unit	L1	Lens (f= -30 mm)
	IF1	Bandpass filter 532-1 nm
	PC1	Polarizing cube beamsplitter
	L2, L3	Lens (f= +30 mm)
	532 // PMT	20 (LC7673)
	P1	Prism
	532 ⊥ PMT	20 (LE0109)
532H, 607 and 1064 nm beam separation unit	L4	Lens (f= +60 mm)
	M7	Longpass filter 560 nm
	IF2	Bandpass filter 532.2-0.7 nm
	L5, ..., L7	Lens (f= +30 mm)
	532H PMT	R9880U-110G (BAE2654)
	M8	Longpass filter 580 nm
	M9	Longpass filter 665 nm (FF665-Di02)
	IF3	Bandpass filter 607.7-1.6 nm
	607 PMT	R9880U-20 (BCC7472)
	IF4	Bandpass filter 1064-4 nm
	1064 PMT	APD 171043-3 mm
289 and 316 nm beam separation unit	L5', ..., L9'	Adaptive lenses
	SM1', ..., SM3'	Spherical mirror
	G1'	3600-line/mm grating
	289 PMT	R1527P
	316 PMT	R1527P

Figure 2: Specifications of LiO3T optics.

Uncertainty source	Equation
Uncertainty due to the Rayleigh calibration value (u_{altref})	$$u_{altref} = \left\lvert \left(\frac{\beta_j}{\beta_N}\right)^2 \frac{U_N}{U_j} \right\rvert \sigma_{\beta_N}$$
Uncertainty due to the lidar ratio value (u_{LR})	$$u_{LR} = \left\lvert \pm p \frac{2\beta_j^2}{U_j} G_j + p^2 \frac{4\beta_j^3}{U_j^2} {G_j}^2 \right\rvert$$ Where: $G_j = \sum_{i=j}^{N} w_i S_i U_i$
Uncertainty due to the SNR vertical distribution (u_{SNR}).	$$u_{SNR} = \sqrt{\left(\frac{\beta_j}{U_j}\right)^2 \sigma_{U_j}^2 + \left(\frac{2\beta_j}{U_j}\right)^2 \sigma_{GU_j}^2}$$ Where: $\sigma_{GU_j}^2 = \sum_{k=j}^{N} (w_k S_k)^2 {\sigma_{U_k}}^2$
Uncertainty due to the SNR value at the calibration altitude ($u_{SNR,altref}$).	$$u_{SNR,altref} \approx \left\lvert \frac{\beta_j^2}{\beta_N U_j} \right\rvert \sigma_{U_N}$$

Table 1: Total-Backscatter analytical error bars from Klett's backward inversion method (from Rocadenbosch et al., 2010).